ELSEVIER

Polymer 41 (2000) 6231–6236

polymer

# Oriented double gyroid films via roll casting

B.J. Dair[a], A. Avgeropoulos[b], N. Hadjichristidis[b], M. Capel[c], E.L. Thomas[a,*]

[a]*Department of Materials Science and Engineering, Massachusetts Institute of Technology, Room 13-5094, 77 Massachusetts Avenue, Cambridge, MA 02139, USA*

[b]*Department of Chemistry, University of Athens, Panepistimiopolis, 157 71 Zougrafou, Athens, Greece*

[c]*National Synchrotron Light Source, Brookhaven National Laboratory, Upton, NY 11973, USA*

Received 23 August 1999; received in revised form 16 November 1999; accepted 16 November 1999

**Abstract**

Films of an isoprene-rich poly (styrene-*b*-isoprene-*b*-styrene) (SIS) triblock copolymer thermoplastic elastomer having a highly textured double gyroid (DG) morphology were produced via roll casting and annealing. The symmetries of the extensional and shear flows involved in the roll casting process are not commensurate with those of the cubic $Ia\bar{3}d$ symmetry of the tricontinuous, triply periodic cubic DG phase. Upon roll casting the microdomain morphology produced is predominantly that of cylinders, oriented with the axes along the roll cast direction. Upon annealing, the DG phase nucleates and grows with the [111] direction oriented along the roll cast direction. The resultant textured films are suitable for investigating the directional dependence of physical properties. © 2000 Elsevier Science Ltd. All rights reserved.

*Keywords*: Double gyroid; Block copolymers; Roll casting

## 1. Introduction

In previous publications we reported the existence of an elastomeric SIS triblock copolymer with an equilibrium double gyroid (DG) morphology [1,2]. Polygranular isotropic films of the DG material have superior stress–strain properties over those of its classical sphere, cylinder, and lamellar counterparts, attributable to the 3D (three-dimension) network structure of the double gyroid. The DG is the only thermoplastic elastomer morphology for which polygranular, isotropic films exhibit necking and drawing. Moreover the DG microdomain structure requires higher stresses for deformation than any of the classical microdomain morphologies, even those having a higher volume percent glassy component [2].

In a glassy-rubbery thermoplastic elastomer system, the double gyroid morphology consists of two glassy networks, each three dimensionally continuous, periodic, and interpenetrating one another without intersection. These glassy networks are embedded in a rubbery matrix, and the overall composite structure has cubic $Ia\bar{3}d$ symmetry. Cubic materials, having the highest symmetry of the crystal classes with only three independent elastic constants, are still elastically anisotropic, since elastic modulus is a fourth rank tensor [3].

The presence of stable necking behavior in the DG morphology suggests a different phenomenological deformation mechanism than the other three-microdomain morphology structures [2]. It is therefore of interest to understand the microstructural deformation mechanisms of this material. In our previous study of the mechanical properties of unoriented DG SIS triblock copolymer films, the overall modulus and deformation behavior were a superposition of that of the variously oriented grains. Therefore, in order to sample any anisotropy in the modulus, strength, and deformation behavior, as well as to probe the detailed microdomain deformation mechanisms, oriented samples need to be produced.

Oriented or textured films of cylindrical or lamellar microdomain morphologies have been produced in the past using extrusion or shear [4–12]. In addition, oriented films can made by the roll-casting process, which orients a material through a combination of shear and extensional flows. The roll-casting orientation technique was developed by Albalak in the Thomas laboratory [13,14]. High-quality, near-single crystal sphere, cylinder, and lamellar morphology films of several types of block copolymer systems, including liquid crystalline blocks and semicrystalline blocks, have been produced by rollcasting diblock and triblock copolymers of the respective compositions

* Corresponding author. Tel.: +1-617-253-6901; fax: +1-617-258-6135.
*E-mail address:* elt@mit.edu (E.L. Thomas).


PII: S0032-3861(99)00847-2

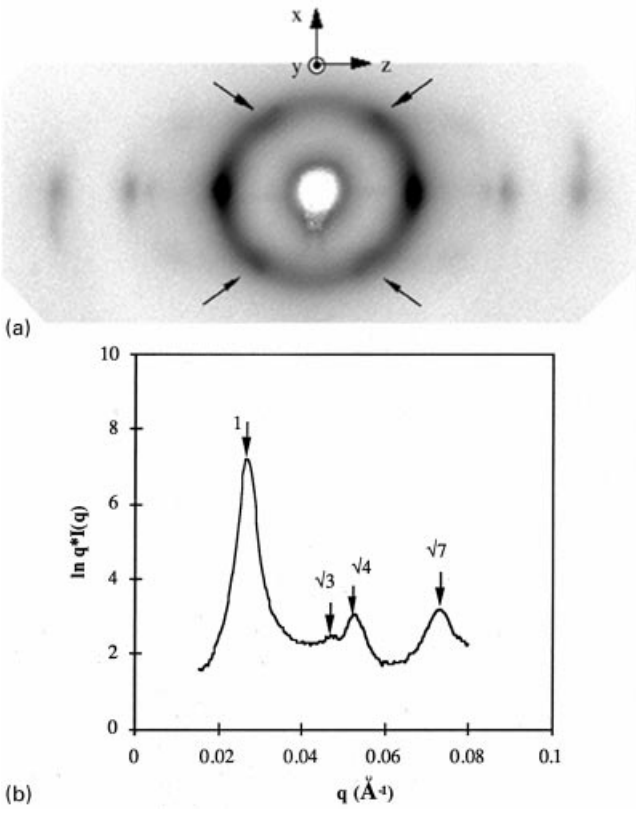


Fig. 1. (a) 2D SAXS pattern of as-roll cast SIS 34, taken in the through-thickness ($y$) direction. The roll cast direction ($x$) is in the vertical. The arrows indicate off-equatorial maxima; (b) 2D radial sector integration 10° around the equator of the SAXS pattern in Fig. 1a. For this composition for a hexagonally packed cylinder microdomain morphology the zero of the form factor is expected at $q \cong 0.044$. The $\sqrt{3}$ peak, occurring at $q = 0.046$, is strongly modulated by the zero of the form factor.

[14–18]. This paper reports on the first use of roll casting to produce a highly textured thermoplastic elastomer with the DG morphology.

## 2. Experimental

A 34 volume per cent (37 wt%) poly(styrene-*b*-isoprene-*b*-styrene) (SIS 34) triblock copolymer with block molecular weights: 13.6–46.4–13.6 k, and PDI = 1.04 forms an equilibrium tricontinuous DG cubic morphology when cast from toluene and annealed [1]. Films of this polymer were made on a roll-caster 1 in. in length, 3/8 in. in diameter, from a concentrated cumene solution (concentration $\approx$ 0.33 g polymer/g solution, with Irganox antioxidant added in amounts $<$1 wt% of the polymer to inhibit degradation) at an angular velocity of 23 rpm and initial gap distance of 0.5 mm. Films were cast in two pourings with the gap distance being increased before each pouring; finished films were first dried for 0.5 h on the roller to allow some of the solvent to evaporate. A cut is then made across the film along the neutral axis and the film is allowed to dry for an additional 2–3 h. Methanol or ethanol, both non-solvents for the polymer, is sprayed along the cut between the polymer film and the steel surface in order to facilitate removal by reducing the surface tension that the polymer has for the roller surface. The films are then flattened between two Teflon® sheets separated by a spacer, giving the film enough room to freely expand or contract, and dried 1–2 days under vacuum to remove all traces of solvent. Films prepared in such a manner without further treatment are referred to as 'unannealed'. Some films were then annealed at 120°C for two weeks under vacuum between the spaced Teflon® sheets and are referred to as 'annealed'.

Small angle X-ray synchrotron experiments were conducted at Brookhaven National Laboratory on beamline X12B using 1.54 Å X-rays and sample-to-detector distances ranging from 247 to 260 cm. Scattering patterns were collected using a custom-built 2D (two-dimensional) detector [19] with 5 min exposure times.

Sections 500–1000 Å thick were prepared by cryomicrotomy at −90°C using a Reichert Jung FC 4E Cryo-ultramicrotome equipped with a diamond knife. TEM samples were picked up on 600 mesh copper grids, and placed in the vapors of 4% osmium tetraoxide-water mixture for 2 h to selectively stain the PI phase. Sections were examined in bright field using a JEOL 2000 FX TEM operated at 200 kV.

Optical transforms (OTs) were taken of the TEM images using an optical diffractometer equipped with a 5 mW polarized UniPhase helium–neon laser with wavelength 633 nm. Diffraction patterns were recorded using Polaroid film. Image areas (from which OTs were taken) were scanned at high resolution (1200–2400 dpi) and fast Fourier transformed (FFT) using NIH Image.

In order to help interpret the sample texture, TEM simulations of the DG structure were made using level surface models [20] on a Silicon Graphics Indigo 2 workstation with the software program TEMsim developed by Hoffman and Hoffman [21]. The level set equation used for a single gyroid network (space group $I4_132$, {110} Fourier component) was: $F(x,y,z) = \sin x \cos y + \sin y \cos z + \sin z \cos x = t$. By taking *pairs* of surfaces $F(x,y,z) = \pm t$ the double gyroid structure with super group $Ia\bar{3}d$ was constructed [22]. For DG surfaces, $t = \pm 1.0$ corresponded to a 34% volume fraction of the minority component networks. Simulations were done for $[\bar{1}10]$ and $[11\bar{2}]$ projections with section thicknesses of one unit cell along the viewing direction.

## 3. Results and discussion

### 3.1. As-roll cast morphology

Fig. 1a shows the 2D SAXS pattern (logarithmic scaling of intensity) of the as-roll cast film of the SIS 34, dried under

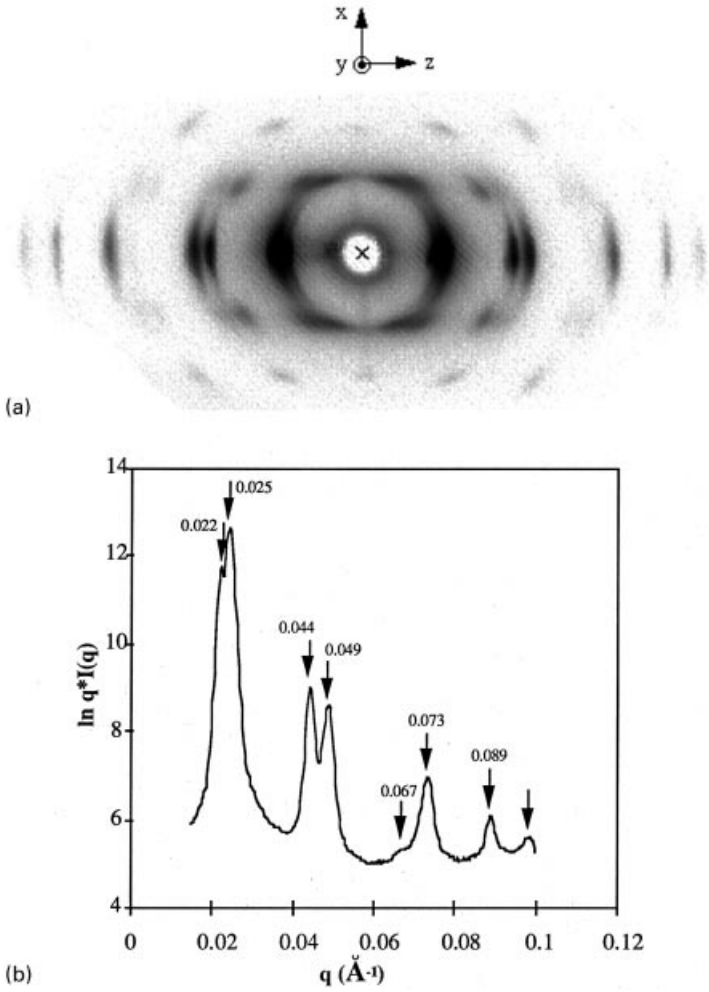


Fig. 2. (a) 2D SAXS pattern with the beam oriented perpendicular to the roll cast film, with the roll cast axis along the vertical; and (b) 2D radial sector integration 10° around the equator of the SAXS pattern in Fig. 2a.

vacuum for one day at ambient temperature. The pattern was taken with the beam through the film thickness direction ($y$), with the roll cast direction ($x$) shown vertical.

Fig. 1b shows a two-dimensional (2D) radial sector integration of the SAXS pattern over a 10° arc centered around the equator. $I(q) \times q$ is plotted versus $q$ as a modified Lorentz correction for an oriented material. Peaks occur at ratios of $q_n/q_1$ of 1.00:1.74:1.97:2.73, indicative of a cylindrical morphology. The first equatorial peak has $q \cong 0.027$ Å$^{-1}$, which corresponds to the (10) planes with a spacing of $d_{10} \cong 230$ Å. The Bragg peaks along the equator of the pattern in Fig. 1a indicate that the cylinders are preferentially oriented along the roll-cast direction. The cylindrical morphology occurs due to the imposed symmetry of the roll-casting process. Other studies have also shown that under a shear field the DG phase is suppressed in favor of cylinders or lamellae [23,24]. Close inspection of the 2D SAXS pattern of the oriented cylinders in Fig. 1a reveals four weak maxima (indicated by arrows) within the continuous ring. The off-equatorial maxima occur at about 50 ± 5° from the equator and therefore do not belong to the oriented cylinder phase (which produces scattering only along the equator). The cylindrical $d_{10}$-spacing is approximately equal to the value of $d_{211}$ of the quiescent-cast SIS 34 [1,25]. These off-equatorial maxima bear resemblance to those pictured in Fig. 2 of Ref. [26], where the oriented lamellar phase undergoes a temperature-induced phase transformation to a complex cubic phase. Since well-annealed films exhibit strong reflections characteristic of the DG phase in this off-equatorial region, this component of the scattering likely arises from a texture comprised of small grains of poorly ordered cubic phase.

### 3.2. Roll cast annealed morphology

Fig. 2a shows the 2D SAXS pattern with the beam through the film thickness direction with the roll cast direction vertical of a film annealed for 2–3 weeks at 120°C. There are 3–4 orders of Bragg peaks along the equator with two additional layer lines of reflections parallel to the equator, indicative of good long range domain order.

Fig. 2b shows a 2D radial sector integration of the SAXS

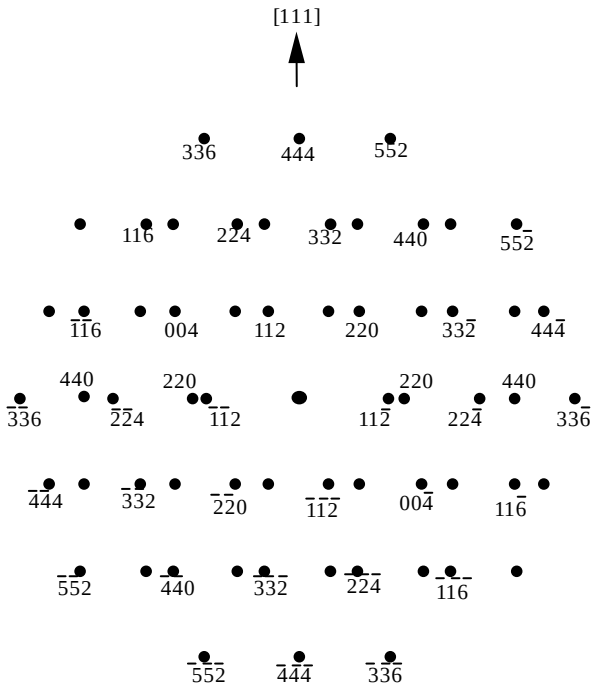


Fig. 3. Indexed scattering pattern of allowed reflections for an $Ia\bar{3}d$ structure with uniaxial symmetry about the [111] direction.

pattern over a 10° arc centered around the equator. An innermost set of two closely spaced reflections occurs in a $q$ ratio of approximately 1.00:1.11, which is close to that expected for the first two reflections of the $Ia\bar{3}d$ DG structure ($\sqrt{8}/\sqrt{6} = 1.155$).

In addition to the SAXS evidence of a DG structure, TEM images of sections cut in different orientations show interconnected and bicontinuous PS and PI domains, atypical of spheres, cylinders, or lamellae. This real-space information also suggests that annealing has produced a textural DG morphology.

### 3.3. Texture of the DG film: SAXS

In both lipid/surfactant/water systems and block copolymer systems the cylinder, double gyroid, and lamellar microdomain morphologies are related "epitaxially" [23,26] and can undergo order–order transitions [27–30]. Rançon and Charvolin determined that the relationships between the phases are as follows:

$$\underset{(001)}{\text{lamellae}} \leftrightarrow \underset{(211)}{Ia\bar{3}d} \leftrightarrow \underset{(10)}{\text{cylinders}}$$

where the respective planes in each phase lie in the same orientation, and their spacings are preserved during the transformation. It was also found that cylinder-to-DG transformations occur directly, whereas the lamellar-to-DG transformations occur via an intermediate hexagonal phase [26,27,30–37].

In the SIS 34 roll cast sample the cylinders are uniaxially aligned along the roll-cast direction. Since in previous surfactant and block copolymer studies the cylinder axes are observed to have an epitaxial relationship with ⟨111⟩ directions of the DG, the ⟨111⟩ direction can be anticipated to align along the roll cast direction. Fig. 3 is a schematic of the allowed reflections for the $Ia\bar{3}d$ structure with uniaxial orientation about the [111] direction. The {211} and {220} reflections account for the strongest peaks observed on both the equator and first layer in the SAXS pattern of the annealed film.

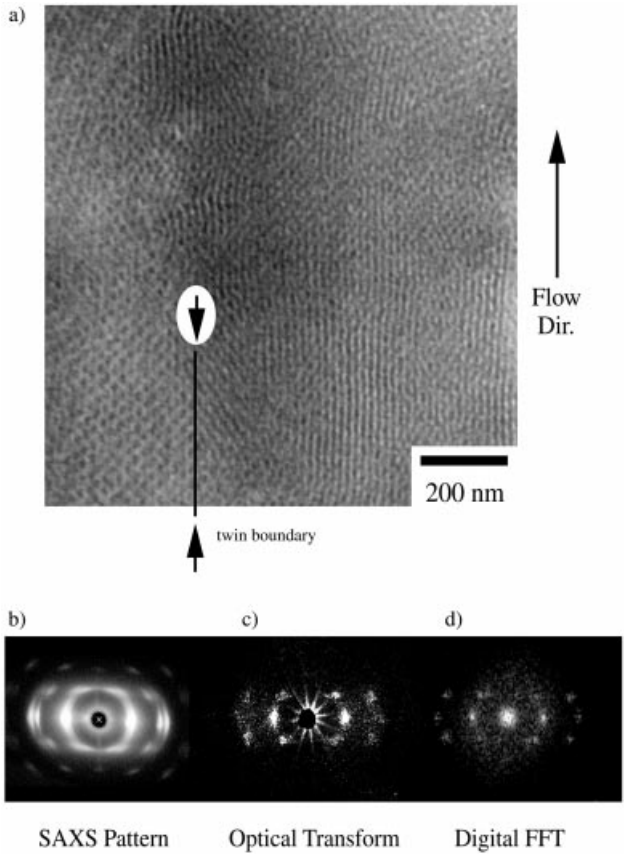


Fig. 4. (a) TEM image of a section cut parallel to the plane of a roll cast annealed SIS 34 film; (b) SAXS pattern with beam oriented perpendicular to the film from which (a) was taken; (c) Optical transform of the TEM image shown in (a); and (d) Fast Fourier Transform of the image in (a). Note good correspondence of all the scattering features in all three scattering patterns.

### 3.4. Texture of the DG film: TEM

Fig. 4a shows a TEM image of roll cast annealed SIS 34. The electron beam is oriented down the same axis as the X-ray beam in Fig. 2b, with the roll cast axis vertical in both. The optical transform and digital fast Fourier transform of the TEM image in Fig. 4a are shown in Fig. 4c–d. Note the rather good correspondence of the features of the SAXS pattern to those present in the image transforms.

The TEM image shows various grains with larger dimensions along the roll cast direction than transverse to it. Three grains can be distinguished across the bottom portion of the

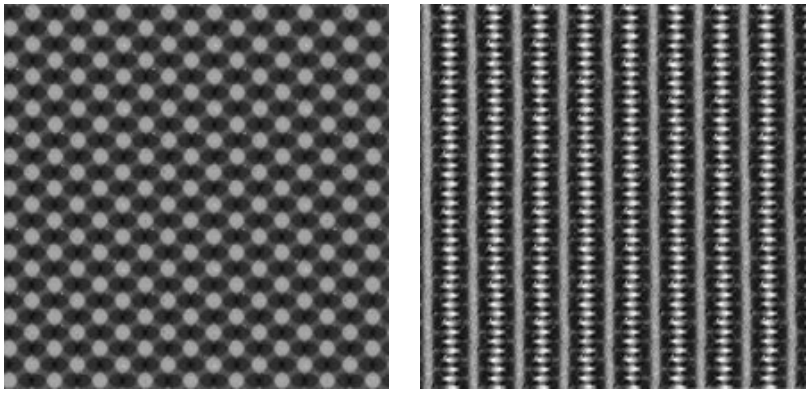

(a) (b)

Fig. 5. TEMsim projections of a level set model of the DG structure with 34% minority networks. The [111] direction is vertical: (a) [$\bar{1}$10]; and (b) [11$\bar{2}$] projections.

image. The image contrast is consistent with $3_1$, and $3_2$ of helices of the PS networks oriented along the roll cast direction. Judging from the images of the different grains, misorientation occurs predominantly around the roll cast axis rather than about an axis normal to the plane of the page. TEMsim projections along [$\bar{1}$10] and [11$\bar{2}$] directions of the DG structure are shown in Fig. 5a and b, respectively. The TEM image in Fig. 5a has areas which resemble the [$\bar{1}$10] projection (lower left-hand corner) and some areas which resemble [11$\bar{2}$] projection (lower right-hand corner). These two types of orientations differ by a 30° rotation around the [111] axis.

## 4. Conclusions

Cubic materials, though having the highest symmetry of the crystal classes, are still mechanically anisotropic. In order to study the directional dependence of the mechanical behavior of the double gyroid, highly textured samples are needed. An isoprene-rich poly(styrene-*b*-isoprene-*b*-styrene) (SIS) triblock copolymer having an equilibrium double gyroid morphology was oriented via roll casting. Because the symmetries of the roll casting process are not commensurate with the cubic symmetry of the DG material, roll casting produces films comprised of cylinders oriented with the axes along the roll cast direction and a portion of small, poorly ordered DG grains. Upon annealing, the equilibrium DG phase nucleates and grows, with the [111] direction along the roll cast direction parallel to the cylinder axes. With such oriented films, the anisotropy of the mechanical properties and deformation behavior of the cubic DG can be studied, which will be presented in subsequent publications [38–39].

## Acknowledgements

We would like to thank Dr Ramon Albalak for the design of the roll caster and Prof. Yachin Cohen, Ariel Eisen, and Chindeum Osuji for helpful scientific discussion. This research was supported by the Air Force (AFOSR F49620-97-1-0385) and by the National Science Foundation (NSF DMR 98-07591).

## References

[1] Avgeropoulos A, Dair BJ, Hadjichristidis N, Thomas EL. Macromolecules 1997;30:5634–42.
[2] Dair BJ, Honeker CC, Alward DB, Avgeropoulos A, Hadjichristidis N, Fetters LJ, Capel MC, Thomas EL. Macromolecules 1999;32:8145–52.
[3] Nye JF. Physical properties of crystals. Oxford: Clarendon Press, 1957.
[4] Dlugosz J, Heller A, Pedemonte E. Colloid Polym Sci 1970;242: 1125–30.
[5] Folkes MJ, Keller A, Scalisi FP. Colloid Polym Sci 1973;251:1–4.
[6] Keller A, Dlugosz J, Folkes MJ, Pedemonte E, Scalisi FP, Willmouth FM. Journal de Physique Colloque C5 1971;32:295–300.
[7] Keller A, Pedemonte E, Willmouth FM. Colloid Polym Sci 1970;238:385–9.
[8] Keller A, Pedemonte E, Willmouth FM. Nature 1970;225:538–9.
[9] Dlugosz J, Folkes MJ, Keller A. J Polym Sci Part B: Polym Phys 1973;11:929–38.
[10] Hadziioannou G, Mathis A, Skoulios A. Colloid Polym Sci 1979;257: 136–9.
[11] Hadziioannou G, Mathis A, Skoulios A. Colloid Polym Sci 1979;257: 15–22.
[12] Hadziioannou G, Skoulios A. Die Makromol Chem Rapid Commun 1980;1:693–6.
[13] Albalak RJ, Thomas EL. J Polym Sci Part B: Polym Phys 1993;31:37–46.
[14] Albalak RJ, Thomas EL. J Polym Sci Part B: Polym Phys 1994;32:341–50.
[15] Honeker CC, Thomas EL. Chem Mat 1996;8:1702–14.
[16] Prasman E, Thomas EL. J Polym Sci Part B: Polym Phys 1998;36:1625–36.
[17] Osuji C, Chen JT, Mao G, Ober C, Thomas EL. Proceedings of the Osaka University Macromolecular Symposia, 1998;9–28.
[18] Park C, Simmons S, Fetters LJ, Hsiao B, Yeh F, Thomas EL. Polymer 2000;41:2971–7.
[19] Capel MC, Smith GC, Yu B. Rev Sci Instrum 1995;66:2295–9.
[20] Lambert CA, Radzilowski LH, Thomas EL. Philos Trans R Soc London A 1996;354:2009–23.
[21] Hoffman J, TEMsim is available at http://www.msri.org/.

[22] Wohlgemuth M, Yufa N, Hoffman J, Thomas EL. Submitted for Publication.
[23] Schulz MF, Bates FS, Almdal K, Mortensen K. Phys Rev Lett 1994;73:86–9.
[24] Hajduk DA, Ho RM, Hilmyer MA, Bates FS, Almdal K. J Phys Chem B 1998;102:1356–63.
[25] Dair BJ. PhD Thesis; Massachusetts Institute of Technology, 1999.
[26] Rançon Y, Charvolin J. J Phys Chem 1988;92:2646–51.
[27] Förster S, Khandpur AK, Zhao J, Bates FS, Hamley IW, Ryan AJ, Bras W. Macromolecules 1994;27:6922–35.
[28] Charvolin J, Sadoc JF. Colloque de Physique 1990;C7:83–96.
[29] Clerc M, Laggner P, Levelut AM, Rapp G. Journal de Physique II (France) 1995;5:901–17.
[30] Hajduk DA, Tepe T, Takenouchi H, Tirrell M, Bates FS, Almdal K, Mortensen K. J Chem Phys 1998;108:1–8.
[31] Vigild ME, Almdal K, Mortensen K, Hamley IW, Fairclough JPA, Ryan AJ. Macromolecules 1998;31:5702–16.
[32] Charvolin J. Contemporary Physics 1990;31:1–17.
[33] Clerc M, Levelut AM, Sadoc JF. Journal of Physics II (France) 1991;1:1263.
[34] Matsen MW. Phys Rev Lett 1998;20:4470–3.
[35] Imai M, Kato T, Schneider D. J Chem Phys 1997;106:9362–71.
[36] Qi S, Wang ZG. Phys Rev E 1997;55:1682–97.
[37] Qi S, Wang ZG. Macromolecules 1997;30:4491–7.
[38] Dair BJ, Avgeropoulos A, Hadjichristidis N, Thomas EL. J Mater Sci 2000; in press.
[39] Dair BJ, Avgeropoulos A, Hadjichristidis N, Capel M, Thomas EL. In preparation.